# Nanofluidics: a pedagogical introduction

*Simon Gravelle*

01 MARCH 2016

## 1 Generalities

### 1.1 What is nanofluidics?

Nanofluidics is the study of fluids confined in structures of nanometric dimensions (typically $1-100\,\mathrm{nm}$) [1, 2]. Fluids confined in these structures exhibit behaviours that are not observed in larger structures, due to a high surface to bulk ratio. Strictly speaking, nanofluidics is not a new research field and has been implicit in many disciplines [3, 4, 5, 6, 7], but has received a name of its own only recently. This evolution results from recent technological progress which made it possible to control what occurs at these scales. Moreover, advances have been made in observation/measurement techniques, allowing for measurement of the *small* physical quantities inherent to nano-sized systems.

Even though nanofluidics is born in the footstep of microfluidics, it would be incorrect to consider it an extension of microfluidics. Indeed, while in microfluidics the only scale which matters is the size of the system, nanofluidics has to deal with a large spectrum of characteristic lengths which induce coupled phenomena and give rise to complex fluid behaviours [8]. Moreover, since nanofluidics is at the intersection between physics, chemistry and biology, it concerns a wide range of domains such as physiology, membrane science, thermodynamics or colloidal science. Consequently, a multidisciplinary approach is often needed for nanofluidics' research.

Some striking phenomena taking place at the nanoscale have been highlighted during the past few years. For example, super-fast flow in carbon nanotubes [9, 10, 11], nonlinear eletrokinetic transport [12, 13] or slippage over smooth surfaces [14] have been measured. Those effects are indicators of the richness of nanofluidics. Accordingly, this field creates great hopes, and the discovery of a large variety of new interesting effects in the next decades is a reasonable expectation. Moreover, one can notice that most of the biological processes involving fluids operate at the nano-scale, which is certainly not by chance [8]. For example, the protein that regulates water flow in human body, called aquaporin, has got sub-nanometric dimensions [15, 16]. Aquaporins are known to combine high water permeability and good salt rejection, participating for example to the high efficiency of human kidney. Biological processes involving fluid and taking place at the nanoscale attest of the potential applications of nanofluidics, and constitute a source of inspiration for future technological developments.

Hereafter, an overview of the current state of nanofluidics is presented. First, a brief state-of-the-art, mainly focused on nano-fabrication and measurement techniques is given. Then some current applications linked to nanofluidics are described.

### 1.2 State-of-the-art

Nanofluidics has emerged from the recent progresses of nanoscience and nanotechnology, such as progresses made in developing nano-fabrication technologies. Fabricating well-controlled channels is a major challenge for nanofluidics, and is a necessary condition for a systematic exploration of nanofluidic phenomena. This requires a good control of device dimensions and surface properties (charge, roughness, etc). For example, the improvement of lithography techniques (electron, x-beam, ion-beam, soft...) allows the fabrication of slit nanochannels [17]. Focus Ion Beam (FIB) allows to drill nanopores in solid membranes [18, 19]. There are also coatings and deposition/etching techniques that can be used to tune the surface properties [20, 21]. Siria et al. were able to manipulate a single boron nitride (BN) nanotube in order to insert it in a membrane separating electrolyte reservoirs and perform electric measurements [22]. Great developments of Scanning Tunneling Mi-

croscope (STM) or Atomic Force Microscopy (AFM) allow to characterize the fabricated devices.

In parallel, the efforts invested in nanofabrication have been combined to an improvement of measurement techniques. Most of them are based on the measurement of electric currents, and have been developed since the early days of physiology. But for a full understanding of nanofluidic properties, other quantities have to be made accessible. For example, local values of a velocity field can be obtained using nano-Particle Image Velocimetry (nano-PIV). Surface Force Apparatus (SFA) have been used to explore the hydrodynamic boundary condition and measure forces that play an important role in nanofluidics, such as van der Waals or electric forces.

In addition, a current challenge concerns water flow measurements. The main difficulty is due to the magnitude of typical flows through nanochannels: $\sim 10^{-18}\,\mathrm{m}^3/\mathrm{s}$ (it would take several years to grow a drop of 1 nl with such a flow). In order to detect a water flow through a nanochannel, some potential candidates have emerged during the last decade. One can cite, for example, Fluorescence Recovery After Photobleaching (FRAP), confocal measurements or coulter counting measurements that have been reported to detect respectively $7 \cdot 10^{-18}\,\mathrm{m}^3/\mathrm{s}$ [23], $10^{-18}\,\mathrm{m}^3/\mathrm{s}$ [24] and $10^{-18}\,\mathrm{m}^3/\mathrm{s}$ [25]. However, the inconvenient of most of the existing measurement techniques is that they are indirect and require the use of dyes or probes.

Meanwhile, numerical progresses combined with calculation capacity improvement allow for the theoretical exploration of a large variety of nanofluidic properties. For example, the friction of water on solid surfaces can be investigated using ab initio methods [26], while molecular dynamics simulations are good candidates for fluid transport investigations [27, 28].

## 1.3 Applications

Some important applications of nanofluidics are listed hereafter.

**Biology** – First of all, most of the biological processes that involve fluids take place at the nanoscale [15, 29, 30, 31]. For example, the transport of water through biological membranes in cells is ensured by aquaporins, a protein with subnanometric dimensions. Aquaporins appear to have an extremely high water permeability, while ensuring an excellent salt rejection [1]. Another example of proteins with nanometric dimensions are ion pumps and ion channels, that ensure the flow of ions across cell membranes [33, 34]. Combined, those proteins allow the (human) kidney, which is an example of natural desalination and separation tool, to purify water with an energy cost far below current artificial desalination plants [8].

**Desalination** – At the same time, some of the most used (man-made) desalination techniques, consisting in the separation of salt and water in order to produce fresh water, are using nanofluidic properties [35, 36]. This is the case of membrane-based techniques, such as Reverse Osmosis (RO) [37], Forward Osmosis (FO) [38] or ElectroDialysis (ED) [39]. The improvement of the membrane technology has made it possible to desalinate with an energy consumption close to the minimum energy set by thermodynamics.

**Extraction of mixing energy** – Another interesting application of nanofluidics concerns the extraction of the energy of mixing from natural water resources. This so-called blue energy is the energy available from the difference in salt concentration between, for example, seawater and river water. Pressure-Retarded Osmosis (PRO) converts the huge pressure difference originating in the difference in salt concentration ($\sim$ bars) between reservoirs separated by a semipermeable membrane into a mechanical force by the use of a semipermeable membrane with nanosized pores [40]. Siria et al. proposed another way to convert blue energy based on the generation of an osmotic electric current using a membrane pierced with charged nanotubes [22].

**Nanofluidic circuitry** – The recent emergence of nanofluidic components benefiting of the surface effects of nanofluidics leads naturally to an analogy with micro-electronics. Indeed, some nanofluidic components imitate the behaviour of over-used microelectronic components such as the diode or the transistor [12] [2]. Even if a complete analogy between both fields fails due to the physical differences between ions and electrons, controlling/manipulating nanoflows the same way we control electric currents would allow for regulating, sensing, concentrating and separating ions and molecules in electrolyte solutions [42] with many potential applications in medicine, such as drug delivery or lab-on-a-chip analyses.

An overview of the full complexity of nanofluidics is highlighted in the following by the description of some theoretical bases. The first part provides the definitions of the characteristic lengths that separate the different transport regimes and lead to a large variety of behaviours. The second part describes

[1] Note that the shape of aquaporins is discussed in reference [32].

[2] Note that nanofluidic diodes are discussed in reference [41].

the numerous forces that play a role in nanofluidics and that are at the origin of the various phenomena. Finally, the third part focuses on transport response of a membrane pierced with a slit nanochannel and submitted to external forcing.

# 2 Definitions

## 2.1 Characteristic lengths

The richness of nanofluidics comes from the existence of a large number of characteristic lengths related to the finite size of the fluid's molecules, to electrostatics or to the fluid dynamics. Indeed, when one or more dimensions of a nanofluidic system compares with those characteristic lengths, new phenomena may appear. An overview of length scales at play in nanofluidics can be seen in figure 1. In what follows, a description of each length is given.

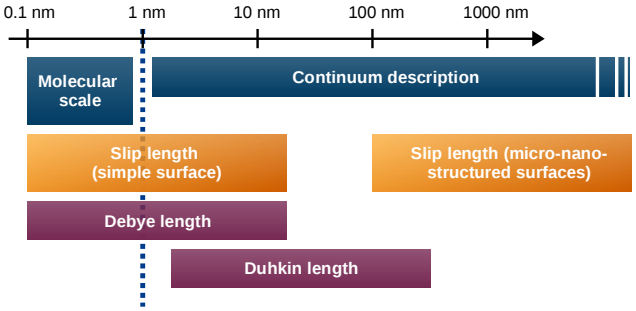


**Figure 1:** Overview of length scales at play in nanofluidics, freely inspired from reference [1].

**The molecular length scale** is associated with the finite size of the fluid's molecules and its components (molecules, ions...). More precisely, it is linked to their diameter $\sigma$, typically in the angstroms scale ($1\,\text{Å} = 1 \cdot 10^{-10}\,\text{m}$). For example, $\sigma \sim 3\,\text{Å}$ for the water molecule, $\sigma \sim 4-5$ Å for common ionic species (Na, K, Cl) [43]. This length defines *a priori* the ultimate limit of the study of nanofluidic transport [1]. In the vicinity of a confining wall, fluids can experience some structuring and ordering at the molecular length scale. An example of water molecules near a solid surface is shown in figure 2. This effect is exacerbated in confining pores, when there is only room for a limited number of molecules. In that case, strong deviations from continuum predictions can be expected. Another important effect related to the size of molecules, and thus to the molecular length is osmosis; which is the phenomenon by which a solvent moves across a semipermeable membrane (permeable to the solvent, but not to the solute) separating two solutions of different concentrations. Note that the question of the robustness of hydrodynamics for confinement below one nanometer and the phenomenon of osmosis are both discussed in my thesis [44].

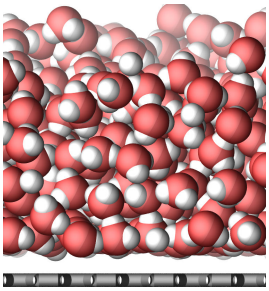

**Figure 2:** Water molecules (oxygen in red, hydrogen in white), next to a graphene sheet (in gray).

**The Bjerrum length** is defined considering two charged species in a solution. It corresponds to the distance at which the thermal energy $k_BT$, with $k_B$ the Boltzmann constant and $T$ the absolute temperature, is equal to the energy of electrostatic interaction. The Bjerrum length $\ell_B$ can be written as

$$\ell_B = \frac{Z^2 e^2}{4\pi\epsilon k_B T}, \tag{1}$$

with $e$ the elementary charge, $Z$ the valency, $\epsilon$ the dielectric permittivity of the medium. For two monovalent species in water at ambient temperature, $\ell_B$ is approximately equal to 0.7 nm. Depending on the considered solution (monovalent ionic species, organic solvent with low dielectric constant, etc.), $\ell_B$ can be either large enough to be clearly dissociated from the molecular length, or be of the same order as the molecular length. The physics has to be differentiated in each case. There are physical effects with important implications on nanofluidic transport that are linked to the Bjerrum length. For example, for confinements below $\ell_B$, one expects a large free-energy cost to undress an ion from its hydration layer and make it enter the pore, with consequences on filtering processes of charged species.

**The Gouy-Chapman length** is constructed in the spirit of the Bjerrum length. It is defined as the distance from a charged wall where the electrostatic interaction of a single ion with the wall becomes of the order of the thermal energy. For a surface charge $\Sigma$, it can be written as

$$\ell_{GC} = \frac{e}{2\pi\Sigma\ell_B}. \tag{2}$$

For monovalent species in water and a typical surface charge $\Sigma \sim 50\ \text{mC/m}^2$, $\ell_{GC}$ is approximately equal to 0.7 nm .

**The Debye length** is the characteristic length of the layer that builds up near a charged surface in an ionic solution. This layer counter balances the influence of the electric charge, and is of main importance in the study of transport at the nanoscale, as will be discussed later. The Debye length can be written as

$$\lambda_D = \frac{1}{\sqrt{8\pi l_B c_0}}, \tag{3}$$

with $c_0$ the concentration in ionic species. Indeed, when a solid surface is immersed in an aqueous solution, it usually acquires a surface charge $\Sigma$ due to chemical reactions (dissociation of surface groups and specific adsorption of ions in solution to the surface [45, 46]). In response to this surface charge, the ionic species in the liquid rearrange themselves and form a layer that screens the influence of the surface charge. This layer of ionic species is called the Electrical Double Layer (EDL). Note that the Debye length is independent of the surface charge $\Sigma$, and inversely proportional to the square root of the salt concentration $c_0$. Typically $\lambda_D$ is equal to 30 nm for $c_0 = 10^{-4}$ M, 3 nm for $c_0 = 10^{-2}$ M and 0.3 nm for $c_0 = 1$ M.

**The Dukhin length** is based on the comparison between the bulk to the surface electric conductance, which links the electric current to an applied electric field. It characterizes the channel scale below which surface conductance dominates over bulk conductance [1]. In a channel of width $h$ and surface charge density $\Sigma$, the excess in counterion concentration is $c_e = 2\Sigma/he$ with $e$ the elementary charge and where the factor 2 accounts for the two surfaces. One may define a Dukhin number $\mathrm{Du} = |\Sigma|/hc_0e$. A Dukhin length $\ell_{\mathrm{Du}}$ can then be defined as

$$\ell_{\mathrm{Du}} = \frac{|\Sigma|}{c_0 e}. \tag{4}$$

For a surface with a surface charge density $\Sigma = 50\,\mathrm{mC/m^2}$, $\ell_{\mathrm{Du}}$ is typically 0.5 nm for $c_0 = 1$ M, while $\ell_{\mathrm{Du}} = 5\,\mu\mathrm{m}$ for $c_0 = 10^{-4}$ M.

**The slip length** is defined as the depth inside the solid where the linear extrapolation of the velocity profile vanishes. Unlike previous lengths, that are all related to electrostatics, the slip length comes from the dynamic of the fluid near a solid surface. It characterizes the hydrodynamic boundary condition of fluids at interfaces. Its expression can be derived as follows: first, assume that the tangential force per unit area exerted by the liquid on the solid surface is proportional to the fluid velocity at the wall $v_w$: $\sigma_{xz} = \lambda v_w$, with $\lambda$ the friction coefficient, $z$ the normal to the surface, $x$ the direction of the flow. Then, combining this equation with the constitutive equation for a bulk Newtonian fluid, $\sigma_{xz} = \eta\partial_z v_x$, one obtains the Navier boundary condition [14]:

$$v_w = \frac{\eta}{\lambda}\partial_z v_x\Big|_w = b\partial_z v_x\Big|_w, \tag{5}$$

where the slip length $b = \eta/\lambda$ is defined as the ratio between the *bulk* liquid viscosity and the *interfacial* friction coefficient. Accordingly, several kinds of hydrodynamic boundary conditions can apply:

- the no-slip boundary condition supposes that the fluid has zero velocity relative to the boundary, $v_w = 0$ at the wall, and corresponds to a vanishing slip length $b = 0$;
- the perfect-slip boundary condition corresponds to the limit of an infinite slip length ($b \to \infty$), or equivalently a vanishing friction coefficient ($\lambda \to 0$). It corresponds to a shear free boundary condition. Traditionally, the perfect-slip boundary condition is used when the slip length $b$ is much larger than the characteristic length(s) of the system;
- the partial-slip boundary condition concerns intermediate slip length.

For simple liquids on smooth surfaces, slip lengths up to a few tens of nanometers have been experimentally measured [14].

## 2.2 Mathematical description of the EDL

The Electrical Double Layer (EDL) plays a fundamental role in nanofluidics due to a large surface area to volume ratio. It corresponds to the layer of ionic species that counter-balances the influence of a surface charge. Numerous phenomena, that will be discussed later, take their origin within the EDL, so a mathematical description of this layer is of main importance here. The conventional description is given hereafter.

**The Gouy-Chapman theory** is at the basis of EDL's description. It is based on the following hypothesis [47]:

- ions are considered as (punctual) spots,
- the dielectric permittivity of the medium is supposed constant in the medium,
- the charge density and the electrical potential are seen as continuum variables,

- the correlations between ions as well as the ion-solvent interactions are not taken into account (mean field theory),
- only electrostatic interactions are considered.

**Poisson-Boltzmann equation** – Under the previous hypotheses, let us write the equation that underlies the distribution of ions near a flat surface. Consider monovalent ions near a flat surface $S$, located at $z = 0$, with homogeneous surface charge density $\Sigma$ and surface potential $V_s$, as shown in figure 3. The link between the electrical potential $V(z)$

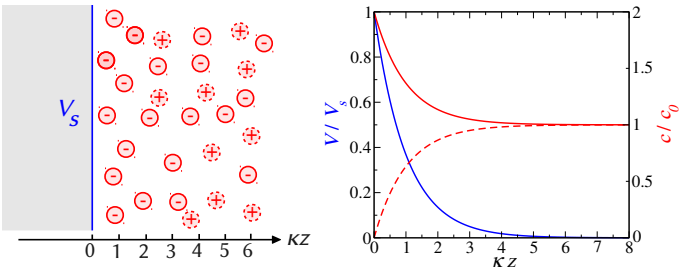


**Figure 3:** Left: scheme of the studied configuration. Right: Debye-Hckel solution (11) for the electrical potential $V$ in blue and linearized Boltzmann equation (12) for the concentration profile $c_\pm$ in red.

and the charge density $\rho_e(z)$ at a $z$ distance of the surface inside the ionic solution is given by a Poisson equation:

$$\Delta V = \frac{\mathrm{d}^2 V}{\mathrm{d}z^2} = -\frac{\rho_e}{\epsilon}, \tag{6}$$

where $\epsilon = \epsilon_0 \epsilon_r$ is the solvent permittivity (for water at ambient temperature, $\epsilon_r \approx 80$). The idea is to ignore the thermal fluctuations of $V$ and $\rho_e$ and to consider their respective averaged values only. At the thermal equilibrium, the densities of positive $c_+(z)$ and negative $c_-(z)$ ions are governed by the Boltzmann equation:

$$c_\pm(z) = c_0 e^{\mp \beta e V(z)}, \tag{7}$$

with $\beta = 1/k_B T$ and $c_0$ the concentration in ion of charge $\pm$ e far from the wall. The charge density reads $\rho_e = e(c_+ - c_-) = -2ec_0 \sinh(\beta e V)$. Coupling this equation with (6), we get the Poisson-Boltzmann equation for the electrical potential $V(z)$:

$$\frac{\mathrm{d}^2 V}{\mathrm{d}z^2} = \frac{2ec_0}{\epsilon} \sinh(\beta e V). \tag{8}$$

Introducing the previously described Bjerrum length $\ell_B$, defined as the length at which the thermal energy balances the electrostatic one, we can rewrite the equation 8:

$$\beta e \frac{\mathrm{d}^2 V}{\mathrm{d}z^2} = 8\pi \ell_B c_0 \sinh(\beta e V) = \kappa^2 \sinh(\beta e V), \tag{9}$$

where $\kappa = (8\pi \ell_B c_0)^{1/2}$ corresponds to the inverse of the previously described Debye length $\lambda_D$. This equation describes the evolution of the electrical potential next to a charged surface.

**Linearized Poisson-Boltzmann equation** – In the general case, the Poisson-Boltzmann equation can not be solved analytically. For small potentials ($eV \ll k_B T$), an approximate form of the Poisson-Boltzmann, the Debye-Hckel equation, can be written as

$$\frac{\mathrm{d}^2 V}{\mathrm{d}z^2} = \kappa^2 V. \tag{10}$$

Assuming that the electrical potential vanishes far from the surface, the solution of the Debye-Hckel equation reads

$$V(z) = V_s e^{-\kappa z}, \tag{11}$$

where $V_s$ is the surface electrical potential. Equation (11) is plotted in figure 3. The electrical potential is screened over a distance $\kappa^{-1} = \lambda_D$, the Debye length, which then gives the width of the EDL. The linearization of the equation (7) gives

$$\begin{aligned} c_\pm &= \rho_s \exp(\mp \beta e V(z)) \approx c_0 (1 \mp \beta e V(z)) \\ &= c_0 (1 \mp \beta e V_s \exp(-\kappa z)). \end{aligned} \tag{12}$$

Equation (12) is plotted in figure 3 for both $\pm$ species.

**Non-linear Poisson-Boltzmann equation** – In some situations, a solution for the non-linear Poisson-Boltzmann equation exists. Let us consider here the case of a single flat wall, the electrolyte is located in $z > 0$ and the solid wall in $z < 0$. A surface charge density $\Sigma < 0$ is located at $z = 0$. The electric field is taken to be equal to 0 inside the wall as well as far from the wall inside the electrolyte. At the wall, the electrostatic boundary condition links the electric field and the surface charge:

$$\left.\frac{\partial V}{\partial z}\right|_{z=0} = -\frac{4\pi}{\epsilon}\Sigma. \tag{13}$$

Solving the PB equation (8) with this boundary condition (13) leads to [48]

$$V(z) = -\frac{2}{e\beta} \ln\left(\frac{1 + \gamma e^{-z/\lambda_D}}{1 - \gamma e^{-z/\lambda_D}}\right), \tag{14}$$

where $\gamma$ is the positive root $\gamma_0$ of the equation:

$$\gamma^2 + \frac{2\ell_{GC}}{\lambda_D}\gamma - 1 = 0. \tag{15}$$

For a positive surface charge $\Sigma$, the solution for $V$ is identical, though with $\gamma = -\gamma_0 (< 0)$. The surface potential $V_s$ can be written as $V_s = 4 \arctan(-z/\lambda_D)/\beta e$.

## 2.3 Nanoscale forces

Now that the general ideas of the Gouy-Chapman description of the EDL have been given, let us describe some of the most important forces that play a role in nanofluidics. These forces are at the origin of the large range of phenomena observed in nanofluidics, and they give rise to both equilibrium or kinetic phenomena [2]. Note that the distinction we will make between forces is artificial since they all are electrical in nature [49], but it still makes sense because of the many different ways in which the electrical force presents itself.

As a side note, each system depends fundamentally on individual forces that are applied between individual atoms. However, in practice, large systems ($\sim 10\,\text{nm}$) can usually be described with continuum theory, which statistically averages the single interactions. This is why we may speak of forces exerted by walls on particles or molecules, or between walls, or between particle or molecules.

**Electrostatic forces** are long range interactions acting between charged atoms or ions [49]. Two particles of respective charges $Q_1$ and $Q_2$ at a distance $r$ act on each other as follows:

$$F(r) = \frac{Q_1 Q_2}{4\pi\epsilon_0\epsilon_r r^2}, \tag{16}$$

where $\epsilon_r$ is the dielectric permittivity of the medium. $F(r)$ is directed along the axis defined by the position of the two particles. Equation (16) is known as the Coulomb law. Electrostatic forces can be either attractive or repulsive, depending on the sign of the product $Q_1 Q_2$. They are, for example, at the origin of the building of the Electrical Double Layer (EDL).

**Van der Waals forces** are residual forces of electrostatic origin which are always present, even between neutral atoms. They are relatively weak in comparison to chemical bonding for example (see below), but they nevertheless play a role in a large range of phenomena such as adhesion, surface tension or wetting. Van der Waals forces even manifest themselves at macroscopic scales since they are at the origin of the adhesion of gecko, a decimetric reptilia, on solid surfaces. Van der Waals forces include attractions and repulsions between atoms, molecules and surfaces. They have three possible origins such as:

- the force between two permanent dipoles,
- the force between a permanent dipole and an induced dipole,
- the force between two induced dipoles (London dispersion force).

Van der Waals forces are long-range, can bring molecules together or mutually align/orient them, and are not additive. They have to be described with the quantum mechanical formalism, which is beyond the scope of the present work.

The DLVO (Derjaguin, Verwey, Landau, Overbeek) theory gives a large picture of nanoscale forces which includes van der Waals forces and coulombic forces. However, some effects that appear at very short range can not be described in the framework of the DLVO theory. Non-DLVO forces are discussed in what follows.

**Chemical or bonding forces** link two or more atoms together to form a molecule [49]. Bonds are characterized by the redistribution of electrons between the two or more atoms. The number of covalent bonds that an atom can form with other atoms depends on its position in the periodic table. This number is called the valency. For example, it is equal to one for hydrogen and two for oxygen, which leads to water molecule $H_2O$ (H-O-H). Notice that covalent bonds are of short range ($0.1 - 0.2\,\text{nm}$) and directed at well-defined angles relative to each other. For example, they determine the way carbon atoms arrange themselves to form diamond structure. Notice that covalent bonding comes from complex quantum interactions which are beyond the scope of the present work.

**Repulsive steric forces** appear when atoms are brought too close together. It is associated with the cost in energy due to overlapping electron clouds (Pauli/Born repulsion). A consequence is the size exclusion, widely used in membranes from angstrm to micrometer [2]. It plays a role for example in aquaporins (water channels), that offer a low resistance for water molecules, but do not allow ions to pass through. To pass through this channel, the ion needs to lose its water shell, which is energetically unfavorable. Notice that, combining electrostatic forces and steric forces, it is possible to develop $K^+$ channels with a high selectivity for $K^+$ over $Na^+$ while both have water shells [50].

**Solvation forces** (or structural forces) are related to the mutual force exerted by one plate on another when they are separated by a structured liquid [3].

[3] Liquid structuring in central in reference [51]

Next to a solid surface, density oscillations are expected. If two solid surfaces immersed in a fluid are separated by a short distance, liquid molecules must accommodate the geometric constraint, leading to solvation forces between the two surfaces, even in the absence of attractive walls. Depending on both surface properties (well ordered, rough, fluid-like) and fluid properties (asymmetrically shaped molecules, with anisotropic or non pair-wise additive interaction potential), the resulting solvation forces can be either monotonic or non-monotonic, repulsive or attractive. See reference [49] for more details. Notice that, in the case of water molecules, solvation forces are called hydration forces.

**Hydrophobic forces** come from interactions between water and low water-soluble objects (molecules, clusters of molecules...). These substances usually have long carbon chains that do not interact with water molecules, resulting in a segregation and an apparent repulsion between water and nonpolar substances. The hydrophobic effect, which results from the presence of hydrophobic forces, is actually an entropic effect: each water molecule can form four hydrogen bonds in pure water, but can not form as much if surrounded by hydrophobic (apolar) species. Hence, apolar molecules (or clusters of molecules) will rearrange themselves in order to minimize the contact surface with water. An example is the mixing of fat and water, where fat molecules tend to agglomerate and minimize the contact with water.

**Non-conservative forces,** such as friction or viscous forces, are referred as non-conservative forces because they involve energy transfer from one body to another. Contrary to other forces, which act on a body and generate a motion according to the second law of Newton, non-conservation forces have no force law and arise as a reaction to motion. Inside a liquid, friction is linked to a fluid property: the viscosity, which is a property of a fluid to resist to a shear. It comes from collisions between neighbouring particles that are moving at different velocities. For example, when a fluid flows through a pipe, the particles generally move quickly near the pipe's axis and slowly near its walls, leading to stress. The friction between water molecules leads to a dissipation that has to be overcome, for example by a pressure difference between the two ends of the pipe, to keep the fluid moving.

**Other forces,** such as gravitational or inertial forces, are of lesser importance in nanofluidics and are not discussed here.

## 2.4 Some consequences

The previously described forces give rise to a large variety of phenomena. As an illustration, some of them are presented here.

**Cohesion** is related to attractive forces between molecules of the same substance. It is due to intermolecular attractive forces. They can be van der Waals forces or hydrogen bonding. Cohesion is at the origin, for example, of the tendency of liquids to resist separation.

**Adhesion** corresponds to attractive forces between unlike molecules. They are caused by forces acting between two substances, which can have various origins, such as electrostatic forces (attraction due to opposite charges), bonding forces (sharing of electron), dispersive (van der Waals forces) etc. For example, water tends to spread on a clean glass, forming a thin and uniform film over the surface. This is because the adhesive forces between water and glass are strong enough to pull the water molecules out of their spherical formation and hold them against the surface of the glass.

**Surface tension** is related to the elastic tendency of liquids which makes them acquire the least surface area possible. This results from the fact that when exposed to the surface, a molecule is in an energetically unfavorable state. Indeed, the molecules at the surface of the liquid lack about half of their cohesive forces, compared to the inner molecules of the bulk liquid [52]. Hence a molecule at the surface has lost about half its cohesion energy. Surface tension is a measure of this lost of energy per surface unit. In the thermodynamic point of view, it is defined as the excess of free energy due to the presence of an interface between two bulk phases [53]. The surface tension $\gamma$ is of the order of magnitude of the bond energy $\epsilon$ between molecules of the fluid divided by the cross section area of a molecule $\sigma^2$:

$$\gamma \sim \frac{\epsilon}{\sigma^2}.$$

Finally one may notice that surface tension is also present at liquid-liquid, liquid-solid and solid-air interfaces.

**Wetting** is the study of the spreading of a liquid deposited on a solid (or liquid) substrate. When a small amount of liquid is put in contact with a flat solid surface, there are two different equilibrium situations: partial wetting, when the liquid shows a finite contact angle $\theta$, and total wetting, in which the liquid spreads completely over the surface and where $\theta$ is not defined. The property of the fluid to spread

on the surface is characterized by the spreading parameter $S$ which measures the difference between the energy per unit area of the dry surface of the solid substrate and the wetted surface:

$$S = \gamma_{SV} - (\gamma_{SL} + \gamma_{LV}) \tag{17}$$

where $\gamma_{SV}, \gamma_{SL}$ and $\gamma_{LV}$ denote the free energies per unit area of respectively the solid-vapour interface, the solid-liquid interface and the liquid-vapour interface equal to the surface tension $\gamma$. In the case of a positive $S$, the surface energy of the dry surface is larger than the energy of the wetted surface, so the liquid tends to extend completely to decrease the total surface energy, hence $\theta$ is equal to zero. A negative $S$ corresponds to a partial wetting situation, where the liquid does not completely spread on the surface and forms a spherical cap, adopting an angle $\theta > 0$. From the equilibrium of the capillary forces at the contact line or from the work cost for moving the contact line, one gets the Young-Dupr relation:

$$\cos\theta = \frac{\gamma_{SV} - \gamma_{SL}}{\gamma}. \tag{18}$$

**Capillary forces** originate in the adhesion between the liquid and the solid surface molecules. It is strongly linked to the existence of a surface tension, as well as to the concept of wetting and contact angle. In certain situations, those forces pull the liquid in order to force it to spread the solid surface. Depending on the configuration, it can make the liquid fill a solid channel for example.

## 2.5 Transport in nanochannels

In this section, we consider various transport phenomena that can occur in a nanochannel separating two reservoirs containing an electrolyte. The purpose is to give a simple expression of each flux as a function of various driving forces (mechanical pressure, solute concentration and electrical potential gradients). For the sake of simplicity, the nanochannel is chosen to be a slit ($\sim$ 2D) and entrance effects are not taken into account [4]. The walls are perpendicular to $z$, respectively located in $z = \pm h/2$ and driving forces are applied along $x$, see figure 4. The channel has a length $L$ along $x$ and a width $w$ along $y$. The Reynolds number $Re = \rho v L/\mu$ (where $\rho$ and $\mu$ are respectively the fluid density and the dynamic viscosity and $v$ and $L$ are respectively the characteristic velocity and length of the flow) is assumed to be lower than one and the problem to be stationary. Hence, the governing equation for the flow is the Stokes equation:

$$\eta \triangle \vec{u} = \vec{\nabla} p + \vec{F} \tag{19}$$

where $\eta$ is the fluid viscosity, $\vec{u}$ is the velocity field, $p$ is the hydrodynamic pressure and $\vec{F}$ a volume force. The surface charge density is $\Sigma$, and will be different from 0 if specified only. Unless otherwise stated, the height of the channel $h$ will be considered large in comparison to the typical range of the potential (i.e. the Debye length). Unless otherwise stated, the no-slip boundary condition will be used for the solvent along walls. The system is shown on figure 4.

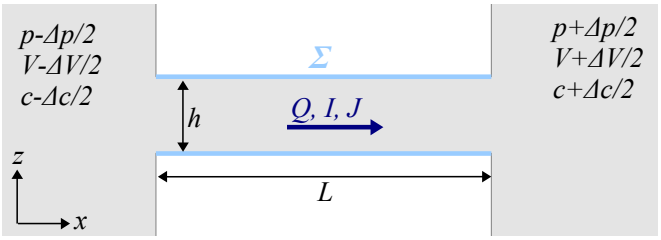


**Figure 4:** Sheme of the 2D channel used for the calculations.

A flow through the membrane can occur as a consequence of a force near the membrane [55]. Here we consider this force to be a mechanic pressure drop $\Delta p$, difference in solute concentration $\Delta c$ or difference in electrical potential $\Delta V$. We suppose that the considered forcing are weak, so equilibrium profiles remain unmodified along z, and flows are linear functions of the forces operating. Hereafter we will study the volume flow $Q$, the ionic flow $J_i$ and the electrical current $I_e$ resulting from $\Delta p$, $\Delta c$ and $\Delta V$. The phenomenological equations linking the three flows to the three forces write:

$$\begin{aligned} Q &= L_{11}\Delta P + L_{12}\Delta c + L_{13}\Delta V, \\ J_i &= L_{21}\Delta P + L_{22}\Delta c + L_{23}\Delta V, \\ I_e &= L_{31}\Delta P + L_{32}\Delta c + L_{33}\Delta V, \end{aligned} \tag{20}$$

where $L_{IJ}$ are coefficients. According to Onsager's law, the matrix of coefficients $L_{IJ}$ is symmetrical, i.e. $L_{IJ} = L_{JI}$. Finally, one assumes that in the middle of the channel ($z$=0), concentration, electrical potential and pressure evolve linearly with $x$.

### Direct terms

The direct terms of the matrix of transport (20) correspond to the diagonal terms $L_{II}$. They link each flux with their natural force, respectively the

[4] Note that hydrodynamic entrance effects are discussed in references [32, 54].

solvent flow with the pressure gradient, the ionic flow with the salt gradient and the ionic current with the electrical gradient. Each of them is calculated hereafter in the previously described configuration (slit nanochannel).

**$L_{11}$ – the hydrodynamic permeability** characterizes the flow transport across a given structure under a pressure gradient. Using both symmetry and impermeability of the walls, one gets for the velocity field: $\vec{u} = u_x(z)\vec{u}_x$. So the Stokes equation 19 can be written as $\eta\partial_z^2 u_x = \partial_x p$. A first integration of the Stokes equation between 0 and $z$ gives $\eta\partial_z u_x = z\partial_x p$, where we used that $\partial_z u_x|_{z=0} = 0$ by symmetry, and that $\partial_x p$ does not depends on $z$. Another integration between $-h/2$ and $z$ using that $\partial_x p = \Delta p/L$ gives

$$u(z) = u_w + \frac{1}{\eta}\left(\frac{z^2}{2} - \frac{h^2}{8}\right)\frac{\Delta p}{L}, \tag{21}$$

where $u_w$ is the wall velocity, which depends on the hydrodynamic boundary condition (see the definition of the slip length, subsection 2.1). Finally, $L_{11}$ in case of the no-slip boundary condition ($u_w = 0$) can be written as

$$\boxed{L_{11} = \frac{Q}{\Delta p} = -\frac{1}{12\eta} \times \frac{wh^3}{L}.} \tag{22}$$

Hence the hydrodynamic permeability of a membrane in the low Reynolds number regime is limited by the viscosity of the fluid, and depends strongly on the dimensions of the channel.

**$L_{22}$ – the ionic permeability** characterizes the ionic flow through a membrane under a salt concentration gradient. From the Fick's law of diffusion:

$$\vec{j}_\pm = -D_\pm \vec{\nabla} c_\pm, \tag{23}$$

where $D_\pm$ are diffusion coefficients of the $\pm$ species respectively, one can write the total flow $J_i$ assuming that $D^+ = D^- = D$:

$$J_i = \int_S (\vec{j}_+ + \vec{j}_-).\mathrm{d}\vec{S} = -wD\int_{-h/2}^{h/2} \partial_x(c_+(x) + c_-(x))\mathrm{d}z. \tag{24}$$

In a neutral channel, and assuming that $c_\pm(x) = x\Delta c/L + c_0$, it gives

$$\boxed{L_{22} = \frac{J_i}{\Delta c} = -D \times \frac{S}{L},} \tag{25}$$

where $S = hw$ is the surface of the channel. Notice that equation (25) describes ionic flow through a membrane under salt gradient in absence of surface charge. In case of the presence of a surface charge density $\Sigma$, the nanochannel exhibits a selective permeability for ion diffusive transport [1]. Consequently, the concentration of counterions inside the channel is higher that the bulk concentration, while the concentration in co-ions is lower. Therefore, ions of the same charge as the nanochannel exhibit a lower permeability, while ions of the opposite charge have a higher permeability through the nanochannel. Following Plesis et al., an effective nanochannel section can be defined for each species $S^\pm_{\text{eff}} = \beta^\pm S$ where $\beta$ is an exclusion/enrichment coefficient [56]:

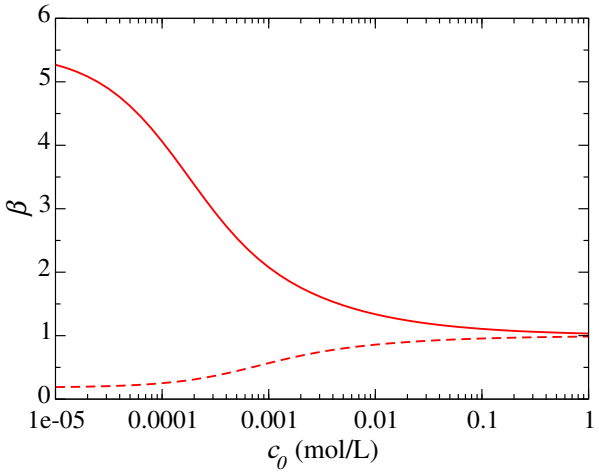


**Figure 5:** Equation (26) for $\beta_+$ (continuous) and $\beta_-$ (dashed) as a function of the bulk concentration for a negatively charged surface.

$$\beta_\pm = \frac{1}{h}\int_{-h/2}^{h/2} e^{\mp\phi(z)}dz; \tag{26}$$

where $\phi(z) = \beta eV(z)$ with $V(z)$ the electrical potential. One can use the linearised Poisson-Boltzmann equation to calculate the ion concentration profile in the slit. An example is shown in figure 5.

**$L_{33}$ – the ionic conductance** characterizes the ionic current through a membrane under an applied electrical potential difference: $G = I_e/\Delta V$. First, let us define the (bulk) conductivity of the solution $\kappa_b$:

$$\kappa_b = e(\mu_+ c_+ + \mu_- c_-) \tag{27}$$

with $\mu_\pm$ and $c_\pm$ respectively the mobility and the volume density of $\pm$ ions [45]. At high ionic strength, or for a neutral channel ($\Sigma = 0$), equation (27) can be used directly to calculate the conductance of the channel $G_{\text{bulk}} = \kappa_b \omega h/L$. However, for a non-neutral channel ($\Sigma \neq 0$), if one looks at the ionic conductance versus the salt concentration on a log-log scale, a conductance plateau is observed at low ionic strength.

This is due to the contribution to the total current of ions of the EDL. This excess counterions concentration can be written as [57]:

$$c_{\rm e} = \frac{2\Sigma}{he} \tag{28}$$

where the 2 accounts for the two surfaces. From this excess counterions concentration, one can define a surface conductance $G_{\rm surf} = e\mu c_{\rm e}\omega h/L$. Then the total conductance is the sum of a bulk conductance and a surface conductance:

$$G = G_{\rm bulk} + G_{\rm surf} = \mu c_s e\frac{wh}{L} + 2\Sigma\mu\frac{w}{L} \tag{29}$$

where we assumed that $\mu_+ = \mu_-$ and defined $c_s = 2c_0$ with $c_0$ the salt concentration. Finally, the ionic current $I_e$ and the voltage drop $\Delta V$ are linked as follows:

$$\boxed{L_{33} = \frac{I_e}{\Delta V} = \mu\left(c_s eh + 2\Sigma\right) \times \frac{w}{L}.} \tag{30}$$

### Cross terms

Additionally to the direct terms, there are cross phenomena coming from couplings between hydrodynamics, ion diffusion and electrostatics. Using statistical mechanics, Onsager has shown the necessity of equality between the term $L_{IJ}$ and $L_{JI}$. So in what follows, only three terms among the six cross coefficients are explicitly calculated, the last three being deduced from Onsager's relation.

**$\mathbf{L}_{13}$ / $\mathbf{L}_{31}$ –** The phenomenon by which a difference of electrical potential $\Delta V$ induces a water flow is called electro-osmosis ($L_{13}$). Its conjugate effect is called streaming current ($L_{31}$) and corresponds to the generation of an electric current by a pressure driven liquid-flow [58]. Hereafter, we will do explicit calculations for the case of electro-osmosis ($L_{13}$).

Electro-osmosis takes its origin in the ion dynamics within the Electrostatic Double Layer (EDL), in which the charge density $\rho_e = e(\rho_+ - \rho_-)$ is non-vanishing. The dynamics of the fluid is described by the stationary Stokes equation with a driving force for the fluid $F_e = \rho_e E_e$, where the electric tangential field $E_e$ is defined as $E_e = -\partial_x V = -\Delta V/L$, and is directed along $x$ [59]:

$$\eta\partial_z^2 u_x + \rho_e E_e = 0. \tag{31}$$

Using that the charge density is linked to the electrostatic potential of the EDL as follows:

$$\rho_e = -\epsilon\frac{\partial^2 V}{\partial z^2}, \tag{32}$$

one finds, after a double integration of the equation (31):

$$u_x(z) = \frac{\epsilon}{\eta}(V(z) - \zeta)E_e \tag{33}$$

where we used the no slip boundary condition and where $\zeta$ is the zeta potential, which is the value of the electrostatic potential at the shear plane, i.e. the position close to the wall where the velocity vanishes [5]. In the no-slip case, the zeta potential is equal to the surface potential $V_s$. As a remark, one can notice that in the case of a finite slip at the wall, characterized by a slip length $b$, the potential $\zeta$ takes the expression:

$$\zeta = V_s \times (1 + b\kappa_{\rm eff}) \tag{34}$$

where $V_s$ is the electrostatic potential at the wall and $\kappa_{\rm eff}$ the surface screening parameter ($\kappa_{\rm eff} = -V'(z = 0)/V_s$). In the case of a weak potential, the screening parameter is approximately equal to the inverse of the Debye length $\lambda_D$. Note that the velocity in the fluid results from a balance between the driving electric force and the viscous friction force at the surface.

An integration of equation (33) gives the following expression for the total water flow:

$$Q = whU_{\rm EO} - \text{surface correction terms}, \tag{35}$$

where $U_{\rm EO}$ is the eletro-osmotic velocity $U_{\rm EO} = -\epsilon\zeta E_e/\eta$. Figure 6 shows a scheme of the velocity

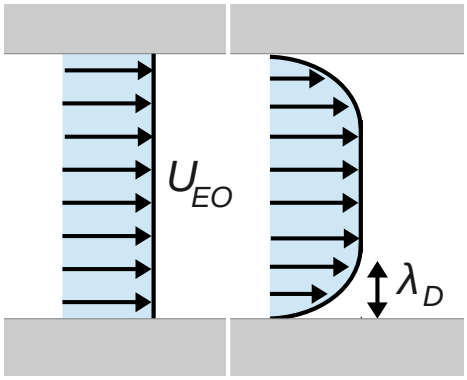


**Figure 6:** Schematic representation of the velocity profile, equation (33) without and with surface correction terms, respectively on the left and on the right.

profile, with and without the surface correction terms. Finally, neglecting the surface correction terms (that

[5] Notice that sometimes the zeta potential is defined as $V_s$ and one has to consider an amplified electro-osmotic mobility to take into account the effect of slippage.

are of the order of $\lambda_D/h \ll 1$), one can write:

$$\boxed{L_{13} = \frac{Q}{\Delta V} \approx \frac{\zeta\epsilon}{\eta} \times \frac{wh}{L}.} \quad (36)$$

Hence electro-osmosis is caused by coulomb force and limited by viscous dissipation.

Accordingly, the streaming current ($L_{31}$), which is the electric current generated by a pressure driven liquid-flow can be written as

$$\boxed{L_{31} = \frac{I_e}{\Delta P} = \frac{\zeta\epsilon}{\eta} \times \frac{wh}{L}.} \quad (37)$$

**$L_{12}$ / $L_{21}$** – The generation of a flow under a solute gradient is called chemi-osmosis ($L_{12}$) [60]. Its conjugate effect is the generation of an excess flux of salt under a pressure drop $\Delta p$ ($L_{21}$). Here the expression of the $L_{12}$ coefficient is obtained in the case of a flow generated by a solute gradient.

So, let us assume the existence of a salt concentration difference $\Delta c$. The salt concentration in the middle of the channel, $c_{\rm mid}(x)$, is assumed to vary linearly along the axis $x$: $c_{\rm mid}(x) = c_0 + \Delta c \times x/L$, where $c_0$ is the concentration in the left reservoir (the concentration in the right reservoir being $c_0 + \Delta c$). From the mechanical equilibrium in $z$ together with the Stokes equation along $z$, one can deduce the hydrostatic pressure profile:

$$p(x,z) = 2k_BTc_{\rm mid}(x)\left[\cosh\phi(x,z) - 1\right] + p_0, \quad (38)$$

where $\phi(x,z) = e\beta V(x,z)$. Injecting this expression in the Stokes equation along $x$, $\eta\partial_z^2 u_x(z) - \partial_x p(x,z) = 0$, one finds:

$$\eta\partial_z^2 u_x(z) = 2k_BT\frac{\Delta c}{L}\left(\cosh\phi - 1\right). \quad (39)$$

Using Poisson-Boltzmann and assuming that $\lambda_D \ll h$, one can find that the flow is:

$$Q = whU_{\rm CO} - \text{surface correction terms}, \quad (40)$$

with $U_{\rm CO}$ the chemi-osmotic velocity:

$$U_{\rm CO} = -\frac{k_BT}{\eta}\frac{\ln(1-\gamma^2)}{2\pi\ell_B}\frac{\Delta c}{c_0 L}, \quad (41)$$

where $\gamma = \tanh(\phi_s/4)$. Neglecting surface correction terms (on the order of $\lambda_D/h \ll 1$), the coefficient $L_{12}$ can be written:

$$\boxed{L_{12} = \frac{Q}{\Delta c} \approx -\frac{k_BT}{\eta c_0}\frac{\ln(1-\gamma^2)}{2\pi\ell_B} \times \frac{wh}{L}.} \quad (42)$$

Chemi-osmosis causes flow towards lower electrolyte concentration. As a complement we will discuss two interesting cases: the case of non-equal diffusion coefficient between + and − species, and the limit of large Debye length $\lambda_D$ compared to the channel height $h$ (this regime is called osmosis).

**Supplement 1** – In the case of a difference in anion and cation diffusivities, an electric field is induced, and a supplementary electro-osmotic contribution has to be taken into account [61]. Assuming a vanishing local current in the outer region and a symmetric electrolyte, this diffusion-induced electric field is proportional to $\beta_0 = (D_+ - D_-)/(D_+ + D_-)$ :

$$E^{\rm D} = \frac{k_BT}{e}\beta_0\frac{{\rm d}\ln c}{{\rm d}x}. \quad (43)$$

So the contribution of this mechanism combined with the previously calculated velocity (equation (41)) gives the following diffusio-osmotic velocity:

$$U_{\rm DO} = -\frac{k_BT}{\eta}\left[\beta_0\zeta\frac{\epsilon}{e} + \frac{\ln(1-\gamma^2)}{2\pi\ell_B}\right]\frac{\Delta c}{c_0 L}, \quad (44)$$

where we used equation (33). The first term corresponds to the electro-osmotic effect, the direction of the generated flow depending on the sign of the product $\beta_0\zeta$, while the second term, called the chemi-osmotic effect, causes a flow towards the lower electrolyte concentration. Neglecting surface correction terms, one can write:

$$\boxed{L_{12} = \frac{Q}{\Delta c} \approx -\frac{k_BT}{\eta c_0}\left[\beta_0\zeta\frac{\epsilon}{e} + \frac{\ln(1-\gamma^2)}{2\pi\ell_B}\right] \times \frac{wh}{L}.} \quad (45)$$

**Supplement 2** – An interesting case is the limit where the Debye length $\lambda_D$ is much larger than the channel height $h$. In this particular case, a constant potential (independent of $z$) called Donnan potential $V_D$ builds up in the entire channel. From the electrochemical equilibrium one gets:

$$\frac{c_+}{c_-} = e^{-2\phi_D}, \quad (46)$$

$$c_+c_- = c_0^2, \quad (47)$$

$$c_+ - c_- = -\frac{2\Sigma}{eh}, \quad (48)$$

where $\phi_D = e\beta V_D$. One can introduce the Dukhin number ${\rm Du} = \Sigma/(ec_0h)$. Then from equation (48), and using that $\cosh^2(x) - \sinh^2(x) = 1$, one gets

$$\cosh(\phi_D) = \sqrt{1 + {\rm Du}^2}. \quad (49)$$

Injecting this expression in equation 39, which has been obtained from mechanical equilibrium in $z$ together with the Stokes equation, one gets

$$Q = -\frac{1}{12\eta}\frac{wh^3}{L} \times \Delta\Pi, \tag{50}$$

where the osmotic pressure $\Delta\Pi$ can be written as

$$\Delta\Pi = 2k_BT\Delta c\left(1+\sqrt{1+\mathrm{Du}^2}\right). \tag{51}$$

Hence, when $\lambda_D \gg h$, one may write

$$\boxed{L_{12} = \frac{Q}{\Delta c} = -\frac{k_BT}{6\eta}\left(1+\sqrt{1+\mathrm{Du}^2}\right) \times \frac{wh^3}{L}.} \tag{52}$$

**$\mathbf{L_{23}}$ / $\mathbf{L_{32}}$** – The current generated under a salt concentration gradient is called osmotic current and the reciprocal effect is the generation of a salt flux under an electrical potential gradient. The expression of $L_{23}$ is here obtained in the first case, i.e. in the case of the generation of current under a salt concentration gradient.

The electrical current $I_e$ can be written as

$$I_e = w\int_{-h/2}^{h/2} e\left(j_+(z) - j_-(z)\right)\mathrm{d}z. \tag{53}$$

Two contributions to the current can be expected, a contribution from the diffusive flux of salt and a contribution from the convective flux of salt. The first one can be written as

$$I_D = w\int_{-h/2}^{h/2} e\left(j_{D,+}(z) - j_{D,-}(z)\right)\mathrm{d}z, \tag{54}$$

with $j_{D,\pm} = -D_\pm\nabla c_\pm$ the diffusive flux of each ion. Assuming that $D = D_+ = D_-$ and rewriting the current as

$$I_D = -ew\partial_x\int_{-h/2}^{h/2}\left(c_+(z) - c_-(z)\right)\mathrm{d}z, \tag{55}$$

$I_D$ appears to be equal to zero from the global charge electroneutrality

$$\Sigma + e\int_{-h/2}^{h/2}\left(c_+(z) - c_-(z)\right)\mathrm{d}z = 0. \tag{56}$$

Accordingly, considering the convective part in equation (53) only, the current can be written as

$$I_e = w\int_{-h/2}^{h/2} e\left(c_+(z) - c_-(z)\right)u_x(z)\mathrm{d}z, \tag{57}$$

where both species $\pm$ move at the same velocity $u_x(z)$ (i.e. there is no electric field along $z$). Using that $\lambda_D \ll h$ (thin electric debye layers as compared to the channel width), one writes:

$$I_e = 2w\int_0^\infty e\left(c_+(z) - c_-(z)\right)u_x(z)\mathrm{d}z. \tag{58}$$

In this assumption, one expects that the entire contribution to the current $I_e$ comes from the convection of ions inside the electric double layers. From the Poisson equation (6), one gets that

$$c_+(z) - c_-(z) = -\frac{\partial^2\phi}{\partial z^2}\frac{1}{4\pi\ell_B}. \tag{59}$$

Moreover, we know from previous section (see equation (39)) that the velocity field $u_x(z)$ under a solute gradient is solution of

$$\eta\frac{\partial^2 u_x}{\partial z^2} = 2k_BT\frac{\Delta c}{L}\left(\cosh\phi - 1\right). \tag{60}$$

Injecting equation (59) in equation (58), performing an integration by part (twice) in the spirit of [62], one gets

$$I_e = \frac{we}{2\pi\ell_B}\left[\phi\frac{\partial u_x}{\partial z}\right]_0^\infty - \frac{we}{2\pi\ell_B}\int_0^\infty \phi\frac{\partial^2 u_x}{\partial z^2}\mathrm{d}z. \tag{61}$$

From equation (60), one get

$$\left.\frac{\partial u_x}{\partial z}\right|_{z=0} = -\frac{2k_BT}{\eta}\frac{\Delta c}{L}\int_0^\infty\left(\cosh\phi - 1\right)\mathrm{d}z. \tag{62}$$

Hence, using that $\phi(z=\infty) = 0$, one gets

$$I_e = -\frac{we}{\pi\ell_B}\frac{k_BT\Delta c}{\eta L}\int_0^\infty(\phi_s - \phi)\times(\cosh\phi - 1)\mathrm{d}z. \tag{63}$$

with $\phi_s$ the normalized surface potential. Using PB equation $\nabla^2\phi = \kappa^2\sinh\phi$, we make the following change of variable:

$$\mathrm{d}z = -\frac{\mathrm{d}\phi}{\kappa\sqrt{2(\cosh\phi - 1)}}, \tag{64}$$

which allows to solve the integral in equation (63). One finds [62]:

$$I_e = 2w\frac{e}{\pi\eta\ell_B}\frac{k_BT}{\kappa}\left(2\sinh\frac{\phi_s}{2} - \phi_s\right)\frac{\Delta c}{L}, \tag{65}$$

that can be rewriten in terms of surface charge (using $2\sinh\phi_s/2 = e\Sigma/\epsilon k_BT\kappa$):

$$I_e = 2w\Sigma\frac{k_BT}{2\pi\eta\ell_B}\left(1 - \kappa\ell_{GC}\,\mathrm{argsinh}\,\frac{1}{\kappa\ell_{GC}}\right)\frac{\Delta c}{Lc_0}, \tag{66}$$

where we have introduce the Gouy-Chapmann length $\ell_{GC} = e/(2\pi\Sigma\ell_B)$. Neglecting the surface correction terms one finds:

$$\boxed{L_{23} = \frac{I_e}{\Delta c} \approx 2w\Sigma \frac{k_B T}{2\pi\eta\ell_B} \frac{1}{Lc_0}} \quad (67)$$

Reciprocally, the flux of salt under electrical gradient can be written as

$$\boxed{L_{32} = \frac{J_i}{\Delta V} \approx 2w\Sigma \frac{k_B T}{2\pi\eta\ell_B} \frac{1}{Lc_0}} \quad (68)$$

### Various comments

We did not give an exhaustive list of phenomena that can occur at the nanoscale. For example thermic effects induced by temperature difference have not been discussed.

Notice that in practice, it is not easy to study each case alone. For example, a channel with a difference of electrical potential, will be subjected to various flux, leading to a charge accumulation at each entrances, i.e. the apparition of an induced salt difference. This is part of the complexity of nanofluidics.

**ACKNOWLEDGMENTS:** S.G. thanks Lydéric Bocquet, Christophe Ybert, Laurent Joly, Benjamin Rotenberg, John Palmeri and Menka Stojanova for usefull comments. This research was supported by the European Research Council programs Micromegas project.

## References

[1] L. Bocquet and E. Charlaix, "Nanofluidics, from bulk to interfaces.," *Chemical Society reviews*, vol. 39, no. 3, pp. 1073–1095, 2010.

[2] J. C. T. Eijkel and A. van den Berg, "Nanofluidics: What is it and what can we expect from it?," *Microfluidics and Nanofluidics*, vol. 1, pp. 249–267, apr 2005.

[3] K. Spiegler and O. Kedem, "Thermodynamics of hyperfiltration (reverse osmosis): criteria for efficient membranes," *Desalination*, vol. 1, no. 4, pp. 311–326, 1966.

[4] F. A. Morrison and J. F. Osterle, "Electrokinetic Energy Conversion in Ultrafine Capillaries," *The Journal of Chemical Physics*, vol. 43, no. 6, 1965.

[5] R. J. Gross and J. F. Osterle, "Membrane Transport Characteristics of Ultrafine Capillaries," *The Journal of Chemical Physics*, vol. 49, no. 1, 1968.

[6] J. C. Fair and J. F. Osterle, "Reverse Electrodialysis in Charged Capillary Membranes," *The Journal of Chemical Physics*, vol. 54, no. 8, 1971.

[7] E. Hoffer and O. Kedem, "Hyperfiltration in charged membranes: the fixed charge model," *Desalination*, vol. 2, no. 1, pp. 25–39, 1967.

[8] L. Bocquet and P. Tabeling, "Physics and technological aspects of nanofluidics.," *Lab on a chip*, vol. 14, no. 17, pp. 3143–58, 2014.

[9] M. Majumder, N. Chopra, R. Andrews, and B. J. Hinds, "Enhanced flow in carbon nanotubes," *Nature*, vol. 438, no. 7064, p. 44, 2005.

[10] J. K. Holt, H. G. Park, Y. Wang, M. Stadermann, A. B. Artyukhin, C. P. Grigoropoulos, A. Noy, and O. Bakajin, "Fast mass transport through sub-2-nanometer carbon nanotubes.," *Science (New York, N.Y.)*, vol. 312, no. 5776, pp. 1034–1037, 2006.

[11] M. Whitby, L. Cagnon, M. Thanou, and N. Quirke, "Enhanced fluid flow through nanoscale carbon pipes," *Nano Letters*, vol. 8, no. 9, pp. 2632–2637, 2008.

[12] H. Daiguji, Y. Oka, and K. Shirono, "Nanofluidic diode and bipolar transistor," *Nano Letters*, vol. 5, pp. 2274–2280, nov 2005.

[13] D. Deng, E. V. Dydek, J. H. Han, S. Schlumpberger, A. Mani, B. Zaltzman, and M. Z. Bazant, "Overlimiting current and shock electrodialysis in porous media," *Langmuir*, vol. 29, no. 52, pp. 16167–16177, 2013.

[14] L. Bocquet and J. L. Barrat, "Flow boundary conditions from nano- to micro-scales," *Soft Matter*, vol. 3, no. 6, pp. 685–693, 2006.

[15] B. L. de Groot and H. Grubmüller, "Water permeation across biological membranes: mechanism and dynamics of aquaporin-1 and GlpF.," *Science (New York, N.Y.)*, vol. 294, pp. 2353–2357, dec 2001.

[16] P. Agre, "Aquaporin water channels," *Bioscience Reports*, vol. 24, no. 3, pp. 127–163, 2005.

[17] D. Mijatovic, J. C. T. Eijkel, and a. van den Berg, "Technologies for nanofluidic systems: top-down vs. bottom-up–a review.," *Lab on a chip*, vol. 5, pp. 492–500, may 2005.

[18] C. Dekker, "Solid-state nanopores.," *Nature nanotechnology*, vol. 2, no. 4, pp. 209–215, 2007.

[19] A. Hemamouche, A. Morin, E. Bourhis, B. Toury, E. Tarnaud, J. Mathé, P. Guégan, A. Madouri, X. Lafosse, C. Ulysse, S. Guilet, G. Patriarche, L. Auvray, F. Montel, Q. Wilmart, B. Plaçais, J. Yates, and J. Gierak, "FIB patterning of dielectric, metallized and graphene membranes: A comparative study," *Microelectronic Engineering*, vol. 121, no. JUNE, pp. 87–91, 2014.

[20] P. Chen, T. Mitsui, D. B. Farmer, J. Golovchenko, R. G. Gordon, and D. Branton, "Atomic layer deposition to fine-tune the surface properties and diameters of fabricated nanopores," *Nano Letters*, vol. 4, pp. 1333–1337, jun 2004.

[21] R. Karnik, C. Duan, K. Castelino, H. Daiguji, and A. Majumdar, "Rectification of ionic current in a nanofluidic diode," *Nano Letters*, vol. 7, no. 3, pp. 547–551, 2007.

[22] A. Siria, P. Poncharal, A.-L. Biance, R. Fulcrand, X. Blase, S. T. Purcell, and L. Bocquet, "Giant osmotic energy conversion measured in a single transmembrane boron nitride nanotube.," *Nature*, vol. 494, pp. 455–8, feb 2013.

[23] A. Cuenca and H. Bodiguel, "Fluorescence photobleaching to evaluate flow velocity and hydrodynamic dispersion in nanoslits," *Lab on a Chip*, vol. 12, no. 9, p. 1672, 2012.

[24] C. Lee, C. Cottin-Bizonne, a. L. Biance, P. Joseph, L. Bocquet, and C. Ybert, "Osmotic flow through fully permeable nanochannels," *Physical Review Letters*, vol. 112, p. 244501, jun 2014.

[25] A. Gadaleta, A.-L. Biance, A. Siria, and L. Bocquet, "Ultra-sensitive flow measurement in individual nanopores through pressure–driven particle translocation," *Nanoscale*, vol. 7, no. 17, pp. 7965–7970, 2015.

[26] G. Tocci, L. Joly, and A. Michaelides, "Friction of water on graphene and hexagonal BN from ab initio methods : very different slippage despite very similar interface structures," *Nano letters*, vol. submitted, 2014.

[27] D. Cohen-Tanugi and J. C. Grossman, "Water desalination across nanoporous graphene," *Nano Letters*, vol. 12, pp. 3602–3608, jul 2012.

[28] W. D. Nicholls, M. K. Borg, D. a. Lockerby, and J. M. Reese, "Water transport through (7,7) carbon nanotubes of different lengths using molecular dynamics," *Microfluidics and Nanofluidics*, vol. 12, pp. 257–264, aug 2012.

[29] M. Borgnia, S. Nielsen, A. Engel, and P. Agre, "Cellular and Molecular Biology of the Aquaporin Water Channels," *Annual Review of Biochemistry*, vol. 68, no. 1, pp. 425–458, 1999.

[30] J. Mathé, A. Aksimentiev, D. R. Nelson, K. Schulten, and A. Meller, "Orientation discrimination of single-stranded DNA inside the alpha-hemolysin membrane channel.," *Proceedings of the National Academy of Sciences of the United States of America*, vol. 102, no. 35, pp. 12377–82, 2005.

[31] A. S. Verkman, "Role of aquaporin water channels in eye function," *Experimental Eye Research*, vol. 76, pp. 137–143, feb 2003.

[32] S. Gravelle, L. Joly, F. Detcheverry, C. Ybert, C. Cottin-Bizonne, and L. Bocquet, "Optimizing water permeability through the hourglass shape of aquaporins.," *Proceedings of the National Academy of Sciences of the United States of America*, vol. 110, pp. 16367–72, sep 2013.

[33] I. M. Glynn, "Annual review prize lecture. 'All hands to the sodium pump'.," *The Journal of physiology*, vol. 462, no. 1, pp. 1–30, 1993.

[34] E. Gouaux and R. Mackinnon, "Principles of selective ion transport in channels and pumps.," *Science (New York, N.Y.)*, vol. 310, no. 5753, pp. 1461–1465, 2005.

[35] N. Ben Amar, H. Saidani, a. Deratani, and J. Palmeri, "Effect of temperature on the transport of water and neutral solutes across nanofiltration membranes," *Langmuir*, vol. 23, no. 6, pp. 2937–2952, 2007.

[36] T. Humplik, J. Lee, S. C. O'Hern, B. a. Fellman, M. a. Baig, S. F. Hassan, M. a. Atieh, F. Rahman, T. Laoui, R. Karnik, and E. N.

Wang, "Nanostructured materials for water desalination.," *Nanotechnology*, vol. 22, p. 292001, jul 2011.

[37] C. Fritzmann, J. Löwenberg, T. Wintgens, and T. Melin, "State-of-the-art of reverse osmosis desalination," *Desalination*, vol. 216, pp. 1–76, oct 2007.

[38] T. Y. Cath, A. E. Childress, and M. Elimelech, "Forward osmosis: Principles, applications, and recent developments," *Journal of Membrane Science*, vol. 281, pp. 70–87, sep 2006.

[39] R. Scheumann and M. Kraume, "Influence of different HRT for the operation of a Submerged Membrane Sequencing Batch Reactor (SM-SBR) for the treatment of greywater," *Desalination*, vol. 248, pp. 123–130, 2009.

[40] A. Achilli, T. Y. Cath, and A. E. Childress, "Power generation with pressure retarded osmosis: An experimental and theoretical investigation," *Journal of Membrane Science*, vol. 343, pp. 42–52, nov 2009.

[41] C. B. Picallo, S. Gravelle, L. Joly, E. Charlaix, and L. Bocquet, "Nanofluidic osmotic diodes: Theory and molecular dynamics simulations," *Physical Review Letters*, vol. 111, no. 24, pp. 1–5, 2013.

[42] W. Guan, R. Fan, and M. a. Reed, "Field-effect reconfigurable nanofluidic ionic diodes," *Nature Communications*, vol. 2, p. 506, jan 2011.

[43] S. Batsanov, "Van der Waals radii of elements," *Inorganic materials*, vol. 37, no. 9, pp. 871–885, 2001.

[44] S. Gravelle, *Nanofluidics: a theoretical and numerical investigation of fluid transport in nanochannels*. PhD thesis, 2015.

[45] R. B. Schoch, J. Han, and P. Renaud, "Transport phenomena in nanofluidics," *Reviews of Modern Physics*, vol. 80, no. 3, pp. 839–883, 2008.

[46] H. Boroudjerdi, Y. W. Kim, a. Naji, R. R. Netz, X. Schlagberger, and a. Serr, "Statics and dynamics of strongly charged soft matter," *Physics Reports*, vol. 416, no. 3-4, pp. 129–199, 2005.

[47] L. Joly, C. Ybert, and L. Bocquet, "Probing the nanohydrodynamics at liquid-solid interfaces using thermal motion," *Physical Review Letters*, vol. 96, no. 4, p. 46101, 2006.

[48] D. Andelman, "Chapter 12 Electrostatic properties of membranes: The poisson-boltzmann theory," *Handbook of Biological Physics*, vol. 1, no. C, pp. 603–642, 1995.

[49] J. N. Israelachvili, *Intermolecular and Surface Forces: Revised Third Edition*. Academic press, 2011.

[50] D. E. Clapham, "Symmetry, Selectivity, and the 2003 Nobel Prize," *Cell*, vol. 115, no. 6, pp. 641–646, 2003.

[51] S. Gravelle, C. Ybert, L. Bocquet, and L. Joly, "Anomalous capillary filling and wettability reversal in nanochannels," *Physical Review E*, 2016.

[52] P.-G. De Gennes, F. Brochard-Wyart, and D. Quéré, *Capillarity and wetting phenomena: drops, bubbles, pearls, waves*. Springer Science & Business Media, 2013.

[53] "The Collected Works of J. Willard Gibbs. Two volumes," *Journal of Chemical Education*, vol. 6, no. 3, p. 591, 1929.

[54] S. Gravelle, L. Joly, C. Ybert, and L. Bocquet, "Large permeabilities of hourglass nanopores : From hydrodynamics to single file transport," *The Journal of Chemical Physics*, vol. 141, p. 18C526, nov 2014.

[55] O. Kedem and A. Katchalsky, "Permeability of Composite Membranes," *Transactions of the Faraday Society*, vol. 59, pp. 1918–1939, 1962.

[56] A. Plecis, R. B. Schoch, and P. Renaud, "Ionic transport phenomena in nanofluidics: Experimental and theoretical study of the exclusion-enrichment effect on a chip," *Nano Letters*, vol. 5, pp. 1147–1155, jun 2005.

[57] H. Daiguji, P. Yang, and A. Majumdar, "Ion Transport in Nanofluidic Circuits," *Nano letters*, vol. 4, no. 1, p. 47405, 2004.

[58] F. H. J. Van Der Heyden, D. Stein, and C. Dekker, "Streaming currents in a single nanofluidic channel," *Physical Review Letters*, vol. 95, p. 116104, sep 2005.

[59] J. Anderson, "Colloid Transport By Interfacial Forces," *Annual Review of Fluid Mechanics*, vol. 21, no. 1, pp. 61–99, 1989.

[60] D. C. Prieve, J. L. Anderson, J. P. Ebel, and M. E. Lowell, "Motion of a particle generated by

chemical gradients. Part 2. Electrolytes," *Journal of Fluid Mechanics*, vol. 148, no. -1, p. 247, 1984.

[61] J. Lee, T. Laoui, and R. Karnik, "Nanofluidic transport governed by the liquid/vapour interface.," *Nature nanotechnology*, vol. 9, pp. 317–23, mar 2014.

[62] A. Siria, P. Poncharal, A.-L. Biance, R. Fulcrand, X. Blase, S. T. Purcell, and L. Bocquet, "Supplementary information: Giant osmotic energy conversion measured in a single transmembrane boron nitride nanotube.," *Nature*, vol. 494, no. 7438, pp. 455–8, 2013.